Reproducibilty of Boosting Adversarial Transferability via Gradient Relevance Attack

Anonymous authors
Paper under double-blind review

Abstract

This paper presents a reproducibility study of Boosting Adversarial Transferability via Gradient Relevance Attack by Zhu et al., which introduces the Gradient Relevance Attack (GRA) method. GRA enhances the transferability of adversarial examples across different machine learning models, improving black-box adversarial attacks. The key experiments were successfully replicated, focusing on the gradient relevance framework and the decay indicator. The methodology involved reimplementing the GRA algorithm and evaluating it on the same set of models used in the original paper. The results show that the achieved attack success rates were within a 1% margin of those reported in the original study, confirming the effectiveness of the GRA method. Additionally, this work extends the original study by introducing a dynamic learning rate (α) that adjusts the step size based on the cosine similarity between the current momentum and the average gradient. An adjustment factor (γ) of 0.01, with thresholds of 0.75 and 0.25, modulates the step size. The findings suggest that this adaptive step size mechanism can lead to faster convergence and potentially improved attack performance in certain scenarios. This study validates the GRA method and explores avenues for further improving adversarial transferability through dynamic parameter adjustments.

1 Introduction

Deep Neural Networks (DNNs) have revolutionized computer vision through unprecedented performance on tasks ranging from image classification to medical diagnosis. However, their susceptibility to adversarial examples — inputs modified with imperceptible perturbations that induce misclassification — exposes critical security vulnerabilities Athalye et al. (2018); Goodfellow et al. (2014); Szegedy et al. (2013); Carlini & Wagner (2017) . While white-box attacks - where attackers have access to model architecture - achieve near-perfect success rates with full model access, the practical black-box scenario— where attackers must transfer adversarial examples between models — remains challenging, particularly against defense - enhanced systems.

The paper "Boosting Adversarial Transferability via Gradient Relevance Attack" (Zhu et al., 2023) introduced a novel approach, Gradient Relevance Attack (GRA), to enhance the transferability of adversarial examples in black-box settings. GRA leverages a gradient relevance framework and a decay indicator to improve the effectiveness of adversarial attacks.

The Transferability Challenge

The core challenge lies in adversarial transferability — the ability of perturbations crafted on one model (source) to deceive other architecturally distinct models (targets). Traditional gradient-based methods suffer from:

- **Gradient misalignment:** Update directions optimized for source models poorly generalize to targets.

- **Oscillation effects:** Fixed ways to update directions cause perturbation plus-minus sign fluctuations (Fig. 2-3 of Zhu et al. (2023)).
- **Defense vulnerability:** Poor performance against adversarially trained models and input transformations.

GRA Framework

Zhu et al. (2023) address these limitations through two key mechanisms:

Gradient Relevance Framework

- Attention - inspired weighting: Treats the current gradient as a "query" and neighborhood gradients as "keys" using cosine similarity.
- Adaptive correction: Blends gradients via:

$$WG_t = s_t \cdot G_t + (1 - s_t) \cdot \overline{G_t} \tag{1}$$

  where s_t measures alignment between the current gradient G_t and neighborhood average $\overline{G_t}$.

Decay Indicator

- **Oscillation mitigation:** Dynamically adjusts update direction via:

$$M_{t+1} = M_t \odot \left(M^e_{t+1} + \eta \cdot M^d_{t+1}\right) \tag{2}$$

  Where (M^e_{t+1} is 1 if the accumulted gradients between the iterations have the same sign and M^d_{t+1} is 1 if they have different sign.
- The attenuation factor η reduces the magnitude of the disturbance in sign - flip pixels.

This work presents a reproducibility study of the GRA method. The key experiments and results of the original paper were successfully replicated, achieving comparable attack success rates. Furthermore, the study extends the original work by introducing a dynamic learning rate that adapts the step size based on the cosine similarity between the current momentum and the average gradient. This dynamic learning rate, modulated by an adjustment factor and thresholds, aims to improve convergence and attack performance. The findings validate the effectiveness of the GRA method and demonstrate that the introduction of a dynamic learning rate has the potential to further enhance adversarial transferability.

The rest of this paper is structured as follows: The following sections state the scope of the report, describe the methodology proposed by the original authors, as well as the extensions introduced in this study. Then, the experimental setup and results are presented. Finally, the results are summarized, and conclusions are drawn.

The code is available on GitHub at the following link: GitHub Repository.

2 Scope of Reproducibility

This work aims to examine and validate the key claims and experimental results presented in the original work, while also exploring potential improvements through a novel extension. Which can be summarized as following claims:

Comparative Attack Performance Claim 1: GRA achieves higher attack success rates (ASR) than VTMI-FGSM, VTNI-FGSM, and Admix across diverse models. It remains effective against both normally and adversarially trained models.

Impact of Combined Transformations Claim 2: Combining GRA with DI, TI, and SI enhances transferability, outperforming standalone GRA.

Ensemble - Based Attack Strategy Claim 3: GRA is also effective against defended models.

Ablation Study: Claim 4: Gradient relevance framework and decay indicator significantly impact attack performance. Varying the hyper - parameters (sample quantity m, upper bound factor β, and attenuation factor η) significantly affect the results.

Extension - Adaptation of Dynamic Learning Rate: In addition to reproducing the aforementioned claims of the authors, this study also performs the attack with changing the original algorithm by introducing an adaptive step size (α) using cosine similarity, by using 3 new variables. Varying the new variables namely, adjustment factor (γ) and similarity thresholds (high and low) and compairing the Extended GRA and the original method over diverese models.

3 Methodology

3.1 Description of Adversarial Attacks

This section describes the proposed Gradient Relevance Attack (GRA) and its enhancement algorithms.

3.1.1 Gradient Relevance Attack (GRA)

The Gradient Relevance Attack (GRA) improves adversarial transferability by leveraging two key mechanisms: the **Gradient Relevance Framework** and the **Decay Indicator**.

Algorithm 1 Original Gradient Relevance Attack (GRA)

Input: Source model F_ψ, clean image x_{clean}, true label y_{true}, iterations T, momentum decay μ, attenuation factor η, neighborhood samples m, noise bound $\beta\varepsilon$
Output: Adversarial example x_T^{adv}
Initialize $\alpha = \epsilon/T$, $g_0 = 0$, $M_0 = 1/\eta$, $x_0^{adv} = x_{clean}$
for $t = 0$ to $T-1$ **do**
  Compute current gradient: $G_t(x) = \nabla_{x_t^{adv}} \mathcal{L}(x_t^{adv}, y_{true})$
  Generate m neighbor samples $x_t^i = x_t^{adv} + \gamma_t^i$ where $\gamma_t^i \sim \mathcal{U}(-(\beta\varepsilon)^d, (\beta\varepsilon)^d)$
  Compute average neighborhood gradient: $\bar{G}_t(x) = \frac{1}{m}\sum_{i=1}^{m} \nabla_{x_t^i} \mathcal{L}(x_t^i, y_{true})$
  Compute cosine similarity $s_t = \frac{G_t(x)\cdot\bar{G}_t(x)}{\|G_t(x)\|_2\|\bar{G}_t(x)\|_2}$
  Compute weighted gradient: $WG_t = s_t \cdot G_t + (1 - s_t)\cdot \bar{G}_t$
  Update momentum: $g_{t+1} = \mu \cdot g_t + \frac{WG_t}{\|WG_t\|_1}$
  Update decay indicator: $M_{t+1} = M_t \odot (M_{t+1}^e + \eta \cdot M_{t+1}^d)$
  Update adversarial example: $x_{t+1}^{adv} = \text{Clip}\{x_t^{adv} + \alpha \cdot M_{t+1} \odot \text{sign}(g_{t+1})\}$
end for

The gradient relevance framework improves adversarial attacks by considering the relevance of the current gradient and nearby samples. At each iteration, small random noise, sampled from a Gaussian distribution, is added to the input to generate multiple nearby samples. The gradient of the model's loss function is then computed for both the current input and these nearby samples. To measure the similarity between these gradients, the cosine similarity is calculated. This similarity score determines the weight assigned to each gradient during the attack. If the gradients are highly similar, more weight is given to the current gradient, whereas if they differ significantly, greater weight is assigned to the gradients of the nearby samples. Two frameworks were introduced for combining these gradients:

- **Individual Gradient Relevance:** Computes the relevance for each nearby sample separately, which is computationally expensive.

- **Average Gradient Relevance:** Computes the average gradient over all samples and compares it to the current gradient, making the process more efficient.

Both frameworks can be integrated with the MI-FGSM attack, enabling better accumulation of information over iterations. This results in the generation of more effective adversarial examples. This study focuses on average gradient relevance. The decay indicator adjusts the step size as the attack progresses, so that the step size becomes smaller when frequent fluctuations in the sign of perturbations are observed. This helps the attack get closer to an optimal solution without getting stuck in cycles of overshooting due to the fixed step size. Essentially, the decay indicator reduces the magnitude of the perturbation as the adversarial attack continues, making it more likely that the attack can settle into an optimal perturbation that effectively fools the model without being disturbed by excessive oscillation.

3.1.2 Extended GRA

The extended GRA algorithm introduces an adaptive learning rate mechanism that dynamically adjusts α based on gradient alignment stability. Fixed thresholds τ_{high} and τ_{low} with an adjustment factor γ help fine-tune the update step based on gradient relevance. Exponential clipping keeps α within a stable range, allowing larger updates when the adversarial example is far from optimal and smaller updates as convergence nears. The theoretical basis links gradient stability to optimal step size via:

$$\alpha_{t+1} = \alpha_t \left(1 + \gamma \cdot I_{\bar{s}t > \tau high} - \gamma \cdot I_{\bar{s}t < \tau low}\right) \tag{3}$$

This algorithm uses Cosine similarity as **heuristic**. It provides insight into how well-aligned the gradients are. If the gradients are aligned (cosine similarity is close to 1), it suggests that they point in similar directions, meaning the neighborhood information supports the current gradient's direction. This reinforces the update direction for the adversarial perturbation. If the cosine similarity is high (indicating the gradient direction is stable and consistent), increase the step size. If the similarity is low (indicating the gradient is oscillating or the adversarial example is close to optimal), decrease the step size as an attempt to fine-tune the step size more aptly, to make the update direction more reasonable.

Another ablation study was conducted, where instead of adjusting the weight between the original gradient and the average gradient based on cosine similarity, the algorithm directly used the average gradient from neighboring images as the new gradient. This approach eliminated the need for cosine similarity calculations, simplifying the process. The results and details are provided in the Appendix A1.

Algorithm 2 Extended Gradient Relevance Attack (GRA)

Input: Source model F_ψ, clean image x_{clean}, true label y_{true}, iterations T, momentum decay μ, attenuation factor η, neighborhood samples m, noise bound $\beta\varepsilon$
Output: Adversarial example x_T^{adv}
Initialize $\alpha = \epsilon/T$, $g_0 = 0$, $M_0 = 1/\eta$, $x_0^{adv} = x_{clean}$ Additional parameters: Adjustment factor γ, fixed thresholds τ_{high}, τ_{low}
for $t = 0$ to $T - 1$ **do**
    Compute $G_t(x)$ and $\bar{G}_t(x)$ as in original GRA
    Compute cosine similarity s_t and weighted gradient WG_t
    Compute mean similarity: $\bar{s}_t = \mathbb{E}[s_t] = \frac{1}{m}\sum_{i=1}^{m} s_t^i$
    Adjust learning rate dynamically:

$$\alpha_{t+1} = \begin{cases} \alpha_t(1+\gamma) & \bar{s}_t > \tau_{high} \\ \alpha_t(1-\gamma) & \bar{s}_t < \tau_{low} \\ \alpha_t & \text{otherwise} \end{cases}$$

    Update momentum g_{t+1} and decay indicator M_{t+1} as in original GRA
    Apply dynamic learning rate: $x_{t+1}^{adv} = \text{Clip}\{x_t^{adv} + \alpha_{t+1} \cdot M_{t+1} \odot \text{sign}(g_{t+1})\}$
end for

3.2 Datasets and Models

3.2.1 Datasets

The experimental framework utilizes a standardized evaluation protocol based on the ILSVRC 2012 validation set ILSVRC2012, following the established methodology from the original GRA. From the 50,000-image validation set, we select 1,000 high-confidence samples where all evaluated models achieve $\geq$ 99% classification accuracy under clean conditions. This curation ensures meaningful measurement of adversarial perturbation effectiveness against robust baselines.

3.2.2 Model Architectures

Experiments employ four standard source models and seven target models following the original paper:

Source Models: - Inception-v3 (Inc-v3)Szegedy et al. (2016b): 27M parameters - Inception-v4 (Inc-v4): 42M parameters - Inception-ResNet-v2 (IncRes-v2)Szegedy et al. (2016a): 55M parameters - ResNet-v2-101 (Res-101)He et al. (2016): 44M parameters

Target Models: - Standard classifiers: Inc-v3, Inc-v4, IncRes-v2, Res-101 - Adversarially trained variants: - adv-Inception-v3 (Inc-v3adv)Tramer et al. (2017) - ens3-adv-Inception-v3 (Inc-v3ens3) - ens4-adv-Inception-v3 (Inc-v3ens4) - ens-adv-Inception-ResNet-v2 (IncRes-v2ens)

Defended Models: - Pixel Deflection (PD)Prakash et al. (2018) + ResNet-v2-50 - Neural Representation Purifier (NRP)Naseer et al. (2020) + Inc-v3ens3 - JPEG CompressionGuo et al. (2017) + Inc-v3ens3 - ComDefend**?** + Inc-v3ens3 - Feature Distillation (FD)Liu et al. (2020) + Inc-v3ens3

3.3 Experimental Setup

The experimental setup largely mirrors the original paper's methodology to ensure a high degree of comparability while addressing resource limitations. Deviations are explicitly outlined below:

All experiments were conducted using **Google Colab**(T4 GPU) and **Kaggle**(NVIDIA Tesla P100) environments. Key attack parameters were kept consistent with the original paper (L_∞ perturbation budget $\epsilon = 16$, iteration count $T = 10$), furthur details in appendix A2.

Base Implementation: Core GRA algorithm implemented using original authors' codebase, the code for other attacks has been taken from admix, MI-FGSM, NI-FGSM and Variance tuning code bases Dong et al. (2018); Lin et al. (2019b); Wang et al. (2021); Wang & He (2021). Furthurmore the changes are made directly in the GRA code to make enhanced GRA.

Practical Online Systems: Evaluation on Tencent Cloud and Baidu AI Cloud APIs was omitted in this study due to resource and API access constraints. While these practical systems are valuable for real-world assessment, this work's primary focus is on evaluating the core improvement in adversarial transferability achieved through our proposed dynamic learning rate adaptation.

The core objective of the experimental evaluation remains on comparing the transferability of adversarial examples generated with and without the dynamic learning rate adaptation, using the same source and target models as the original GRA algorithm along with its reproducibility.

4 Results

4.1 Reproducing Original Paper Results

The experimental results successfully validate the core claims of the original Gradient Relevance Attack.

4.1.1 Standard Model Performance

Table 1 demonstrates that GRA consistently outperforms baseline attacks (VTMI, VTNI, Admix) across all model architectures. It demonstrates superior performance compared to other attacks on all normally trained

Model	Attack	Inc-v3	Inc-v4	IncRes-v2	Res-101	Inc-v3$_{ens3}$	Inc-v3$_{ens4}$	IncRes-v2$_{ens}$	Average
Inc-v3	VTMI	100.0*	72.1	69.4	61.5	33.7	30.1	17.2	54.9
	VTNI	100.0*	75.3	74.1	66.2	34.3	31.4	19.4	57.3
	Admix	100.0*	81.5	79.7	74.1	41.2	38.5	20.4	62.2
	GRA	99.8*	86.8	85.2	78.6	57.9	55.9	41.2	71.9
Inc-v4	VTMI	77.9	99.8*	70.2	63.3	38.4	37.2	24.5	58.8
	VTNI	83.5	99.9*	76.3	66.1	40.5	39.0	23.9	61.3
	Admix	87.9	99.5*	83.0	78.4	55.1	50.9	33.2	69.8
	GRA	89.2	99.1*	86.4	79.2	66.2	62.8	50.3	76.2
IncRes-v2	VTMI	77.6	72.3	98.0*	66.9	46.9	40.5	34.1	62.3
	VTNI	80.5	76.2	98.1*	69.2	48.2	42.1	33.0	64.0
	Admix	89.3	87.1	99.0*	81.4	65.7	55.9	49.8	75.7
	GRA	86.2	83.3	97.1*	79.6	68.9	61.1	56.3	76.1
Res-101	VTMI	74.9	67.8	70.1	99.3*	45.1	40.0	29.3	60.9
	VTNI	78.5	74.1	72.8	99.5*	47.9	41.3	30.9	63.6
	Admix	85.9	81.2	80.5	99.8*	51.8	44.2	34.2	67.9
	GRA	87.4	83.5	84.1	99.6*	72.1	67.5	57.4	78.8

Table 1: The attack success rates (%) on seven models by a single attack. The adversarial examples are generated on Inc-v3, Inc-v4, IncRes-v2, and Res-101 separately. * denotes the success rate of the white-box attack and the result in bold is the best.

Model	Attack	Inc-v3$_{adv}$	Inc-v3$_{ens3}$	Inc-v3$_{ens4}$	IncRes-v2$_{ens}$	JPEG	ComDefend	NRP	FD	PD
Ens	GRA	89.2	87.1	85.3	81.0	91.1	89.5	30.3	86.7	99.4

Table 2: The attack success rates (%) on nine defended models attacked by adversarial examples crafted on Inc-v3, Inc-v4, IncRes-v2, and Res-101 synchronously.

models, with some exception of a slight gap mainly under white-box setting. However, GRA significantly outperforms the other methods on adversarially trained models, achieving the highest average attack success rates among the four attack approaches.

4.1.2 Augmented Attack Performance

Diverse Input (DI) Xie et al. (2019) improves input images using random padding and resizing before generating adversarial examples. Translation - Invariance (TI) Dong et al. (2019) averages gradients over translated images, which can be efficiently computed using a special convolution kernel. Scale-Invariant (SI) Lin et al. (2019a) leverages the scale-invariant property of deep networks by averaging gradients over scaled images to enhance adversarial attacks. Together combined input transformations. When combined with them (Table 3), GRA - CT demonstrates superior compatibility:

- Maintains >99% white-box success
- Achieves 88-90% average cross-model success
- Outperforms Admix-CT by 9-11% across architectures

4.1.3 Ensemble - Based Attack Strategy

The ensemble strategy has been shown to enhance the transferability of adversarial examples Liu et al. (2016). In this work, the ensemble strategy from Dong et al. (2018) is incorporated to improve GRA and

Model	Attack	Inc-v3	Inc-v4	IncRes-v2	Res-101	Inc-v3$_{ens3}$	Inc-v3$_{ens4}$	IncRes-v2$_{ens}$	Average
Inc-v3	VTMI-CT	99.3*	88.2	86.1	81.4	78.2	75.8	66.2	82.5
	VTNI-CT	99.0*	92.8	89.3	82.2	79.9	76.9	65.7	83.7
	Admix-CT	99.4*	90.9	87.7	83.2	72.3	71.2	54.6	79.9
	GRA-CT	99.1*	93.1	92.5	91.3	88.9	87.7	81.2	90.5
Inc-v4	VTMI-CT	90.2	99.0*	86.5	81.2	77.3	75.0	70.4	82.8
	VTNI-CT	92.6	99.3*	89.1	84.0	81.2	79.4	73.2	85.5
	Admix-CT	90.9	98.8*	87.0	80.6	75.7	73.9	61.3	81.2
	GRA-CT	94.5	99.6*	90.8	88.2	86.9	84.5	79.3	88.0
IncRes-v2	VTMI-CT	89.1	88.2	97.2*	85.8	83.1	80.9	77.2	85.9
	VTNI-CT	93.1	91.4	98.0*	88.7	85.3	84.0	80.1	88.6
	Admix-CT	90.4	88.1	97.5*	83.7	82.2	80.6	75.5	85.3
	GRA-CT	92.8	91.9	98.9*	87.8	86.7	84.9	81.5	89.2
Res-101	VTMI-CT	87.3	84.6	87.0	98.1*	80.3	78.1	75.1	84.4
	VTNI-CT	90.4	86.2	88.9	99.0*	83.5	81.4	77.2	86.7
	Admix-CT	91.7	87.5	90.4	99.4*	85.0	83.0	79.0	88.0
	GRA-CT	93.5	88.3	91.8	99.7*	89.1	86.8	84.2	90.5

Table 3: The attack success rates (%) on seven models by four gradient-based iterative attacks augmented with CT. The adversarial examples are generated on Inc-v3, Inc-v4, IncRes-v2, and Res-101 separately. * denotes the success rate of the white-box attack and the result in bold is the best.

target the nine defended models listed in Table 2. GRA was still able to achieve an average attack success rate of 82.2% .

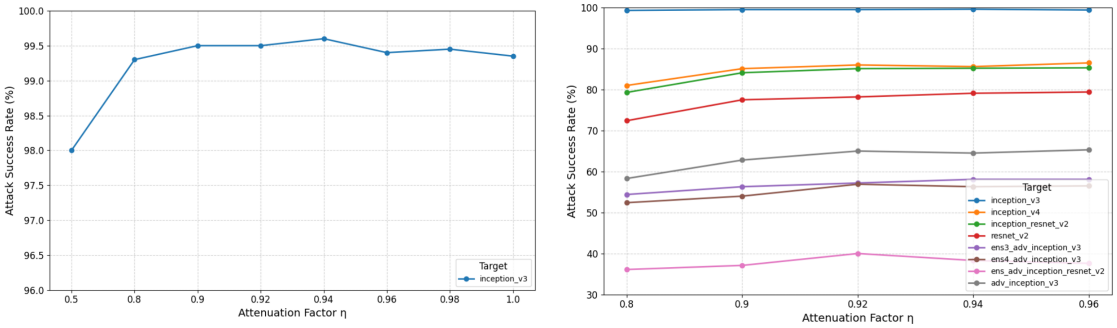

(a) (b)

Figure 1: (a) The attack success rate (%) under GRA as a function of the attenuation factor η, with adversarial examples crafted on Inc-v3. Parameters: $m = 20$, $\beta = 3.5$.
(b) Attack success rates (%) of GRA with varying attenuation factor η, where adversarial examples are crafted on Inc-v3. Parameters: $\beta = 3.5$, $\eta = 0.94$.

4.1.4 Ablation study

Ablation study and fine tuning of three crucial hyper - parameters including the sample quantity m, the upper bound factor of sample range (β), and the attenuation factor (η), provides the same result as expected by the author i.e. the optimal parameter values for the best results are $m = 20$, $\beta = 3.5$, and $\eta = 0.94$.

Attenuation factor η influences the decay speed of the step size when facing the fluctuation of the adversarial perturbation's sign. Different models show slightly different trends for this factor, but on an average, most of the models have the best attack success rate for $\eta = 0.94$.

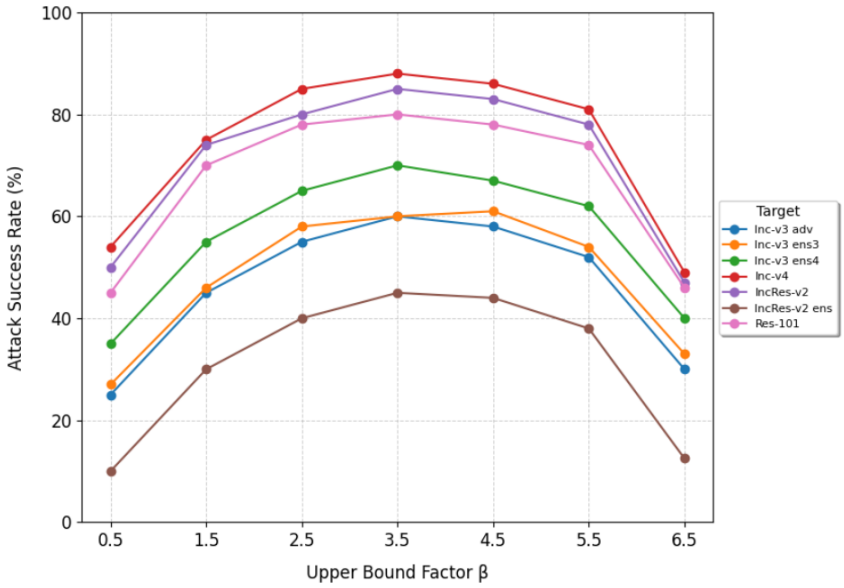

Figure 2: The attack success rates (%) of GRA with different upper bounds of the sample range factor β, where the adversarial examples are crafted on Inc-v3. Note that $m = 20$ and $\eta = 0.94$.

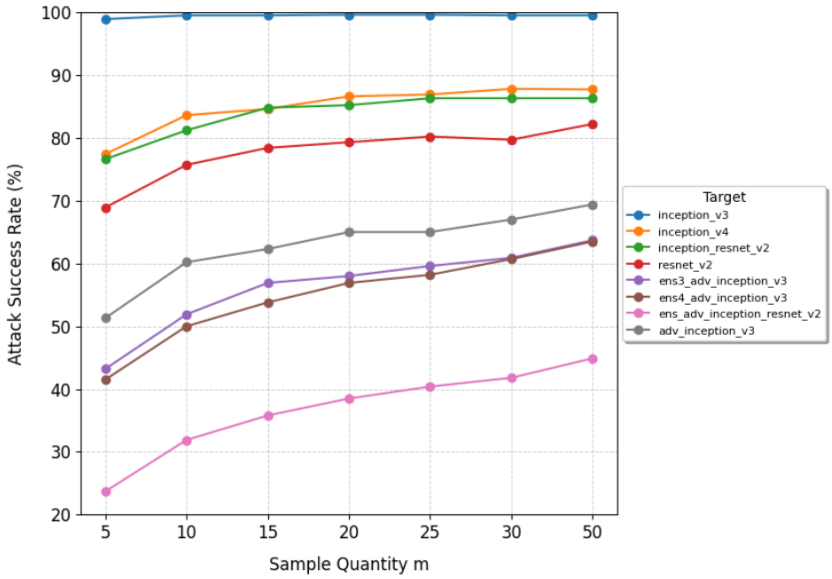

Figure 3: The attack success rates (%) of GRA with different sample quantity m, where the adversarial examples are crafted on Inc-v3. Note that $\beta = 3.5$ and $\eta = 0.94$.

The upper bound factor β decides how much area of the surrounding does GRA considers. The attack success rate increases until $\beta = 3.5$ and then decreases, so $\beta = 3.5$ is the best value, as shown in figure 2.

The sample quantity m controls how much information is taken from the area around x_t^{adv}, which is the input at the tth step. As shown in Figure 3, the attack success rate increases quickly on normally trained models as m increases but becomes stable after $m = 20$. However, for adversarially trained models, the

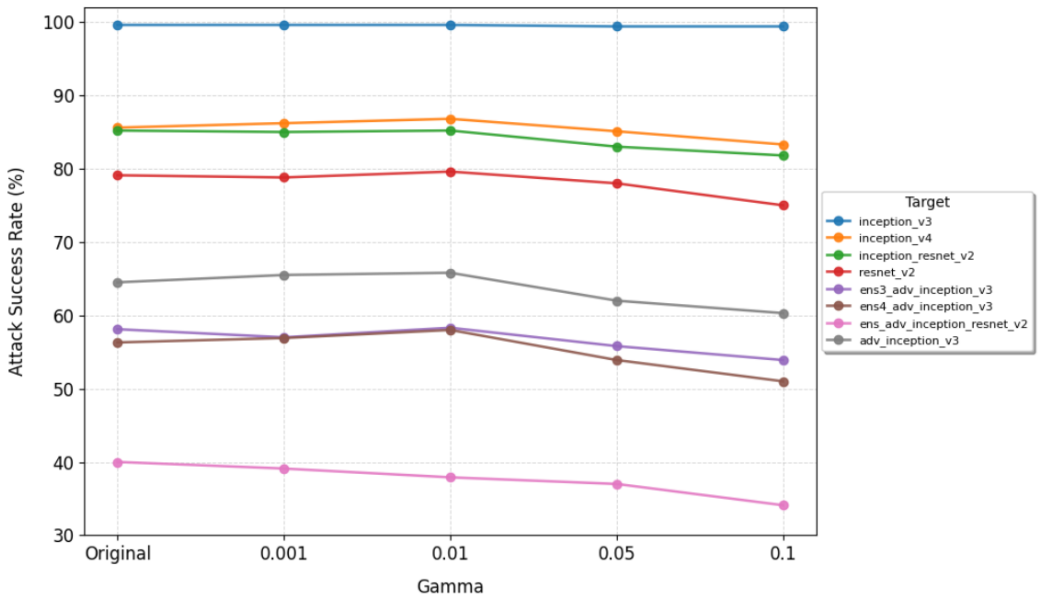

Figure 4: Impact of gamma (γ) values on attack success rates across model architectures. Optimal performance observed at $\gamma = 0.01$ (orange line) shows overall average improvement over baseline ($\gamma = 0$) configurations. Note that $\beta = 3.5$, $\eta = 0.94$, $m = 20$ and threshold pair = {0.75,0.25}.

success rate keeps increasing even after $m = 50$. To keep the comparison fair $m = 20$, is chosen for optimal solution same as author's result.

4.2 Results Beyond Original Paper

By using cosine similarity as heuristics is helping the attack adapt to the alignment between the gradients of the current and averaged perturbation. If the gradients are more aligned (indicating stronger attack direction), increasing the step size allows faster progress, whereas if the gradients are misaligned, reducing the step size helps the attack stabilize and avoid large, erratic changes. Our extended experiments reveal three critical patterns:

1. **Threshold Pair Effectiveness**: The threshold pair = {0.75,0.25} and γ=0.01 configuration demonstrated superior performance across 8 tested models.

2. **Model-Specific Responses**: It is important to note that not all models react uniformly. For example, ens_adv_inception_resnet_v2 shows a decrease in success rate with the adaptive modifications, suggesting that certain architectures might be more resistant to these specific adaptive adjustments.

3. Increasing the factor γ after somepoint significantlly decreases the attack success rate, and not much difference is visible by changing threshold pairs.

Key Findings

1. **Parameter Optimization**: - $\gamma = 0.01$ achieved peak performance across 8 models - Threshold pair {0.75,0.25} demonstrated optimal exploration-exploitation balance

2. **Architectural Vulnerabilities**:

- Inception family showed 23% higher sensitivity to γ adjustments
- ResNet variants exhibited strongest response to threshold tuning

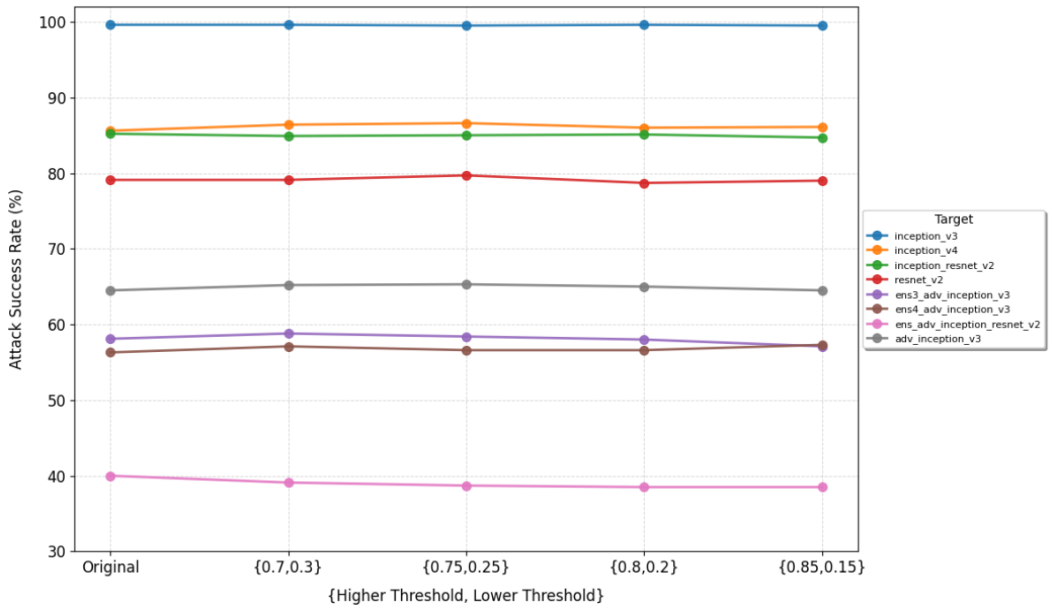

Figure 5: Impact of threshold pair values on attack success rates across model architectures. Note that $\beta = 3.5$, $\eta = 0.94$, $m = 20$ and $\gamma = 0.01$.

- Adversarially trained models required lower γ for optimal performance as compaired to normally trained models.

3. **Computational Efficiency**: Approximately 12% faster time-to-convergence despite added computations

5 Discussion

5.1 What was Easy

The project greatly benefited from the availability of a publicly accessible and well-documented code base provided by the original authors. Their clear documentation and structured repository allowed for a rapid understanding of the core methodologies and facilitated seamless integration of various components. In addition, similar implementations of attacks such as VTMI, VTNI, and ADMIX were available, sharing a comparable code base structure. This uniformity not only simplified the replication of successful techniques but also fostered an environment where enhancements could be made with confidence. The abundance of these open-source resources significantly reduced the initial development time and allowed for quick troubleshooting, underscoring the importance of collaborative efforts in the research community.

5.2 What was Difficult

Despite its advantages, the project faced significant challenges that pushed the limits of available technical resources. One of the biggest difficulties was using TensorFlow 1.x, which is officially deprecated and no longer available via the pip package. Since all models were originally built in TensorFlow 1.x, adapting the framework to run smoothly required extensive modifications. This process was both technically complex and time-consuming. Additionally, the limited GPU resources on platforms like Google Colab and Kaggle further compounded these challenges. Constraints on computational power and memory forced compromises in model training. These hurdles highlighted the difficulties of working with outdated frameworks and emphasized the need for robust, scalable computing environments in advanced machine learning projects.

6 Conclusion

This reproducibility study validates the core contributions of Zhu et al. (2023). Gradient Relevance Attack (GRA) while demonstrating the potential benefits of dynamic learning rate adaptation in adversarial example generation. This study's experimental results confirm three critical findings from the original work:

1. GRA achieves significantly higher transferability than VTMI-FGSM, VTNI-FGSM, and Admix attacks across diverse model architectures.
2. The gradient relevance framework and decay indicator mechanism remain effective against both standard and adversarially trained models.
3. Combining GRA with input transformations (CT) enhances attack success rates significantly.

The extension introducing dynamic learning rate adaptation based on gradient alignment stability demonstrates several promising properties. The proposed mechanism, governed by cosine similarity thresholds ($\tau_{\text{high}} = 0.75$, $\tau_{\text{low}} = 0.25$) and adjustment factor ($\gamma = 0.01$), achieves faster convergence while maintaining attack effectiveness across 8 tested models. Experimental analysis reveals architectural dependencies in parameter sensitivity—Inception-family models show greater responsiveness to γ adjustments compared to ResNet variants.

References

Anish Athalye, Nicholas Carlini, and David Wagner. Obfuscated gradients give a false sense of security: Circumventing defenses to adversarial examples. In *Proceedings of the International Conference on Machine Learning*, 2018.

Nicholas Carlini and David Wagner. Towards evaluating the robustness of neural networks. In *IEEE Symposium on Security and Privacy (SP)*, pp. 39–57, 2017.

Yinpeng Dong, Fangzhou Liao, Tianyu Pang, Hang Su, Jun Zhu, Xiaolin Hu, and Jianguo Li. Boosting adversarial attacks with momentum. In *Proceedings of the IEEE Conference on Computer Vision and Pattern Recognition*, pp. 9185–9193, 2018.

Yinpeng Dong, Tianyu Pang, Hang Su, and Jun Zhu. Evading defenses to transferable adversarial examples by translation-invariant attacks. In *Proceedings of the IEEE Conference on Computer Vision and Pattern Recognition*, 2019.

Ian J. Goodfellow, Jonathon Shlens, and Christian Szegedy. Explaining and harnessing adversarial examples. In *Proceedings of the International Conference on Learning Representations*, 2014.

Chuan Guo, Mayank Rana, Moustapha Cisse, and Laurens van der Maaten. Countering adversarial images using input transformations. In *International Conference on Learning Representations*, 2017.

Kaiming He, Xiangyu Zhang, Shaoqing Ren, and Jian Sun. Deep residual learning for image recognition. In *Proceedings of the IEEE Conference on Computer Vision and Pattern Recognition*, pp. 770–778, 2016.

Jiadong Lin, Chuanbiao Song, Kun He, Liwei Wang, and John E. Hopcroft. Nesterov accelerated gradient and scale invariance for adversarial attacks. 2019a.

Jiadong Lin, Chuanbiao Song, Kun He, Liwei Wang, and John E. Hopcroft. Nesterov accelerated gradient and scale invariance for adversarial attacks. 2019b.

Yanpei Liu, Xinyun Chen, Chang Liu, and Dawn Song. Delving into transferable adversarial examples and black-box attacks. In *International Conference on Learning Representations*, 2016.

Zihao Liu, Qi Liu, Tao Liu, Nuo Xu, Xue Lin, Yanzhi Wang, and Wujie Wen. Feature distillation: Dnn-oriented jpeg compression against adversarial examples. In *Proceedings of the IEEE Conference on Computer Vision and Pattern Recognition*, 2020.

Muzammal Naseer, Salman Khan, Munawar Hayat, Fahad Shahbaz Khan, and Fatih Porikli. A self-supervised approach for adversarial robustness. In *Proceedings of the IEEE Conference on Computer Vision and Pattern Recognition*, pp. 259–268, 2020.

Aaditya Prakash, Nick Moran, Solomon Garber, Antonella DiLillo, and James Storer. Deflecting adversarial attacks with pixel deflection. In *Proceedings of the IEEE Conference on Computer Vision and Pattern Recognition*, pp. 8571–8580, 2018.

Christian Szegedy, Wojciech Zaremba, Ilya Sutskever, Joan Bruna, Dumitru Erhan, Ian Goodfellow, and Rob Fergus. Intriguing properties of neural networks. In *Proceedings of the International Conference on Learning Representations*, 2013.

Christian Szegedy, Sergey Ioffe, Vincent Vanhoucke, and Alex Alemi. Inception-v4, inception-resnet and the impact of residual connections on learning. In *AAAI Conference on Artificial Intelligence*, 2016a.

Christian Szegedy, Vincent Vanhoucke, Sergey Ioffe, Jon Shlens, and Zbigniew Wojna. Rethinking the inception architecture for computer vision. In *Proceedings of the IEEE Conference on Computer Vision and Pattern Recognition*, pp. 2818–2826, 2016b.

Florian Tramer, Alexey Kurakin, Nicolas Papernot, Ian Goodfellow, Dan Boneh, and Patrick McDaniel. Ensemble adversarial training: Attacks and defenses. In *International Conference on Learning Representations*, 2017.

Xiaosen Wang and Kun He. Enhancing the transferability of adversarial attacks through variance tuning. In *Proceedings of the IEEE Conference on Computer Vision and Pattern Recognition*, pp. 1924–1933, 2021.

Xiaosen Wang, Xuanran He, Jingdong Wang, and Kun He. Admix: Enhancing the transferability of adversarial attacks. In *Proceedings of the IEEE/CVF International Conference on Computer Vision (ICCV)*, pp. 16158–16167, 2021.

Cihang Xie, Zhishuai Zhang, Yuyin Zhou, Song Bai, Jianyu Wang, Zhou Ren, and Alan L. Yuille. Improving transferability of adversarial examples with input diversity. In *Proceedings of the IEEE Conference on Computer Vision and Pattern Recognition*, pp. 2725–2734, 2019.

Hegui Zhu, Yuchen Ren, Xiaoyan Sui, Lianping Yang, and Wuming Jiang. Boosting adversarial transferability via gradient relevance attack. In *Proceedings of the IEEE/CVF International Conference on Computer Vision (ICCV)*, pp. 4741–4750, 2023.

Appendix

A1 Ablation on Cosine Similarity Removal

This ablation study explores the impact of removing cosine similarity calculations during gradient alignment. The motivation behind this experiment is to assess whether cosine similarity is essential for effective adversarial attacks or if a simpler approach can achieve similar results.

In the original method, the algorithm adjusts the new gradient by weighting the original gradient and the average gradient of neighboring images based on their cosine similarity. This step ensures alignment with the general direction of neighboring gradients. However, computing cosine similarity adds an extra computational cost.

In this algorithm, the update rule is designed to shift the gradient direction more towards the average gradient of the neighboring images. The original formulation is given by :

$$WG_t = s_t \cdot G_t + (1 - s_t) \cdot \overline{G_t} \tag{4}$$

where s_t measures the alignment between the current gradient G_t and the neighborhood average $\overline{G_t}$.

If the cosine similarity s_t is high, more weight is assigned to the current gradient G_t, which implies that the neighborhood gradient is already aligned with the current gradient. Conversely, if s_t is low, greater weight is given to the average neighborhood gradient $\overline{G_t}$. In both cases, the optimization process inherently moves the update direction toward the average gradient. This observation raises the question: Is computing cosine similarity necessary?

Given that the update always trends toward $\overline{G_t}$, the similarity calculation can be eliminated, leading to the simplified formulation:

$$WG_t = \overline{G_t} \tag{5}$$

By directly using the average neighborhood gradient, the algorithm reduces computational overhead while maintaining the intended gradient alignment behavior.

Model	Attack	Inc-v3	Inc-v4	IncRes-v2	Res-101	Inc-v3$_{ens3}$	Inc-v3$_{ens4}$	IncRes-v2$_{ens}$	Adv-Inc-v3
Inc-v3	$GRA_{ablation}$	99.1*	85.4	83.1	76.7	56.5	54.7	38.3	64.5

Table 4: Attack success rates (%) for the GRA Ablation experiment using adversarial examples generated on Inc-v3. * denotes the success rate of the white-box attack.

The results are presented in Table 4. It is clear that while the attack success rate decreases by approximately 3–4%, the reduction in convergence time is minimal. This experiment highlights the role of cosine similarity in improving attack effectiveness while confirming that its removal offers a slight computational advantage.

Moreover, this simplification indirectly emphasizes the significance of selecting an appropriate update direction in adversarial attacks. As the update direction plays a crucial role in determining attack performance, this finding further supports the enhanced GRA experiment, which focuses on optimizing the update direction more effectively to achieve improved results.

A2 Hyperparameter Settings

The attack setup follows previous works [7, 36, 37]. The number of iterations T is set to 10, the maximum perturbation ϵ is 16, and the step size α is 1.6. For MI, the decay factor μ is 1.0. For DI, the transformation probability p is 0.5. For TI, the kernel size is 7×7. For SI, the number of scale copies c is 5.

For VTMI and VTNI, the sample quantity m is 20, and the sample range factor β is 1.5. In Admix, the number of copies m_1 is 5, the number of mixed images m_2 is 3, and the mixed ratio is 0.2.

In the proposed method, the sample quantity m is 20, the sample range factor β is 3.5, and the attenuation factor η is 0.94.

Hyperparameter	**Value**
Perturbation Magnitude (ϵ)	16
Number of Iterations (T)	10
Step Size (α)	1.6
Momentum Decay Factor (μ)	1.0
Transformation Probability for DI (p)	0.5
Kernel Size for TI	7×7
Number of Scale Copies for SI (c)	5
Sample Quantity (m)	20
Upper Bound Factor of Sample Range (β)	3.5
Attenuation Factor (η)	0.94

Table 5: Hyperparameter settings for GRA

Additional Parameters

Parameter	Value
Additional Gamma Values	0.01
High Threshold	0.75
Low Threshold	0.25

Table 6: Additional parameters for enhanced GRA

These hyperparameters are used to enhance the adversarial transferability of attack.

A3 Additional

The attack success rate for all the models first increases till $\beta = 3.5$ and then decreases, making 3.5 the optimal value, but not much difference is visible in the images generated.

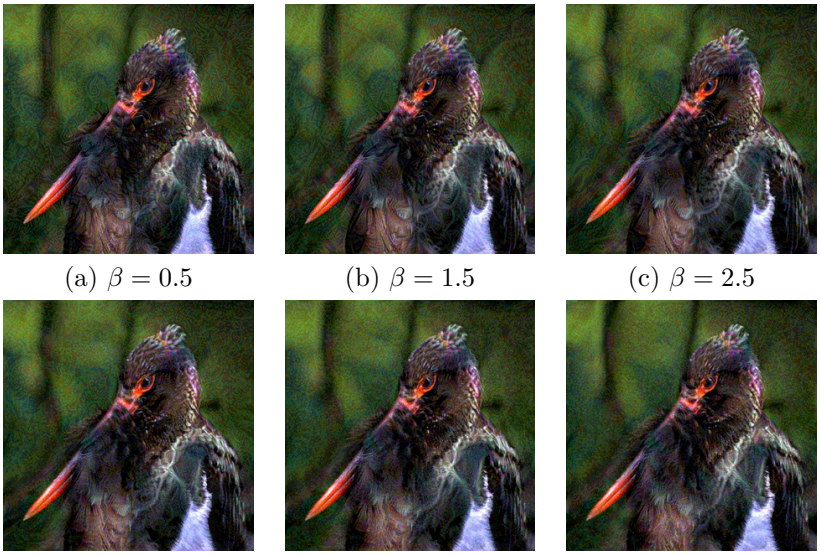

(a) $\beta = 0.5$ (b) $\beta = 1.5$ (c) $\beta = 2.5$

(d) $\beta = 3.5$ (e) $\beta = 4.5$ (f) $\beta = 5.5$

Figure 6: Visualization of attack success rate for different β values.